Domains within Domains and Walls within Walls: Evidence for Polar Domains in Cryogenic $SrTiO_3$

E. K. H. Salje,* O. Aktas, and M. A. Carpenter
Department of Earth Sciences, University of Cambridge, Downing Street, Cambridge CB2 3EQ, United Kingdom

V. V. Laguta
Institute of Physics AS CR, Cukrovarnicka 10, 16200 Prague, Czech Republic

J. F. Scott
Department of Physics, University of Cambridge, Cambridge CB3 0HE, United Kingdom
(Received 13 August 2013; published 11 December 2013)

Resonant piezoelectric spectroscopy shows polar resonances in paraelectric $SrTiO_3$ at temperatures below 80 K. These resonances become strong at $T < 40$ K. The resonances are induced by weak electric fields and lead to standing mechanical waves in the sample. This piezoelectric response does not exist in paraelastic $SrTiO_3$ nor at temperatures just below the ferroelastic phase transition. The interpretation of the resonances is related to ferroelastic twin walls which become polar at low temperatures in close analogy with the known behavior of $CaTiO_3$. $SrTiO_3$ is different from $CaTiO_3$, however, because the wall polarity is thermally induced; i.e., there exists a small temperature range well below the ferroelastic transition point at 105 K where polarity appears on cooling. As the walls are atomistically thin, this transition has the hallmarks of a two-dimensional phase transition restrained to the twin boundaries rather than a classic bulk phase transition.

DOI: 10.1103/PhysRevLett.111.247603 PACS numbers: 77.80.B−, 68.35.Rh, 77.80.Dj, 77.84.Cg

Strontium titanate, with its subtle and complex phase transitions, was once described by Nobel prize-winner Alex Müller [1] as the ''drosophila of solid state physics,'' after the ubiquitous fruit fly whose many changes of structure formed the basis for much of modern genetics. And despite literally hundreds of publications on it, its low-temperature behavior still remains quite enigmatic.

Spurred on by a strong resemblance between the non-monotonic wave vector dependence of its acoustic phonon branch, which strongly resembles roton dispersion in liquid helium, plus a kink in its order parameter temperature dependence near 35 K, Müller proposed ''super'' properties of SrTiO3 [1] (also Ref. [2]); these are now viewed as arising from more pedestrian origins and not super at all. Shortly thereafter Courtens *et al.* [3,4], based upon a small unexplained splitting in transverse acoustic phonon energies, proposed the existence of second sound in the same temperature range [5], the present consensus is that this arises from small displacements of Sr ions along [111] directions that lower the tetragonal symmetry below ~70 K and remove vibrational mode degeneracies. But the strontium titanate saga continues, exacerbated or enhanced by the ferroelectricity of O-18 $SrTiO_3$ and by the novel superconductivity of semiconducting strontium titanate of both oxygen isotopes [6]. The interest in the properties of $SrTiO_3$ at very low temperatures has recently been enhanced by the discovery that its structure is not the centrosymmetric $D4h$ known since 1968 [7], but a triclinic structure created by small Sr displacements along [111] directions convoluted with the oxygen-octahedron counter-rotations (locally this structure will be acentric with point group symmetry 1, but globally it may average to a centered $\bar{1}$ symmetry). This may have serious implications for superconductivity in $SrTiO_3$, a subject of recently renewed interest. First, it means that the superconductivity is in a material lacking inversion symmetry, which in turn implies spin-triplet mechanisms [8]. Second, the symmetry lowering from tetragonal to triclinic below ~60 K complicates the band structure and thereby relates to the newly discovered ''dome structures'' in the superconducting phase diagram [9]. Even in the tetragonal phase above ~60 K strontium titanate exhibits light- and heavy-electron bands, but the triclinic distortion will split them by crystal fields into xy-like, yz-like, and zx-like subbands. (In CdS the light and heavy hole bands are p like, deriving from the oxygen $2P$ states, and hence are x or y like with a hexagonal crystal field. However, in $SrTiO_3$ the heavy electrons are d like, originating from Ti d states, and lowering the symmetry from tetragonal to triclinic below ~60 K will introduce an additional splitting.) Third, the Sr-[111] disorder will produce a huge increase in the optical phonon density of states available for Cooper pairs at $T < 60$ K, not yet considered in models of $SrTiO_3$ superconductivity. And finally, as shown in the present Letter, $SrTiO_3$ single crystals exhibit ferroelectric polarization, at least locally.

In order to understand the effect of microstructures it is crucial to realize that $SrTiO_3$ is perhaps unique among

ferroelastic materials in the fact that ferroelastic twin walls in the tetragonal phase remain highly mobile under externally applied stress at all temperatures down to at least 15 K [10]. More normal behavior would involve the twin walls becoming pinned and immobile at some low temperature, as typified for example by $LaAlO_3$ [11]. Here we bring together these two strands of remarkable effects, i.e., the unique twin wall mobility and the local instabilities relating to the proximity to a ferroelectric transition. The key ingredient is the observation that weak, high-frequency electric fields lead to large elastic resonances at temperatures below 80 K with a major effect below 40 K. This sudden appearance of polarity is understood to be located in the ferroelastic domain walls because there is no indication that the bulk of the materials suddenly becomes piezoelectric. Wall related polarity was anticipated by Salje *et al.* [12] and polar twin walls were recently observed in structurally closely related $CaTiO_3$ [13,14]. There have been several earlier indications that microstructures in $SrTiO_3$ are polar. The first relates to grain boundaries [15]. More recently, a similar suggestion was made for twin boundaries by Zubko *et al.* [16]. To our knowledge the present observations are the clearest indication yet that wall polarity exists in $SrTiO_3$ at low temperatures. Relaxing the structural constraints at 0 K by *ab initio* simulations [17] has claimed massive piezoelectricity in a hypothetical orthorhombic phase which we do not confirm in this study (the piezoelectric effect was speculated to be larger than in piezoelectric quartz).

To detect the weak polarity in $SrTiO_3$, we have developed an experimental technique, labeled resonant piezoelectric spectroscopy, RPS. The experimental arrangement in Fig. 1 involves the application of an ac voltage across the sample. The applied voltage leads to the oscillation of domain boundaries through the piezoelectric effect in the sample, which creates strain fields proportional to the electric field [18]. The resulting elastic wave becomes resonant if its frequency corresponds to one of the natural frequencies of the sample. What makes RPS sensitive to microscopic or macroscopic polar ordering is this mechanical resonance condition, which enhances the amplitude of the elastic wave enormously. Resonant elastic standing waves, (i.e., mechanical resonances), are then detected using a piezoelectric transducer, similar to resonant ultrasonic spectroscopy (RUS) [19,20]. As both RPS and RUS excite the mechanical resonances of the sample, one would expect an overlap of some of the resonance frequencies. However, the mechanism for the excitation of elastic waves is quite different in the two techniques: RPS uses the piezoelectric effect inherent to the sample to excite elastic resonances, in RUS these resonances are mechanically excited using an emitter transducer, which would be in contact with the top corner of the sample in Fig. 1.

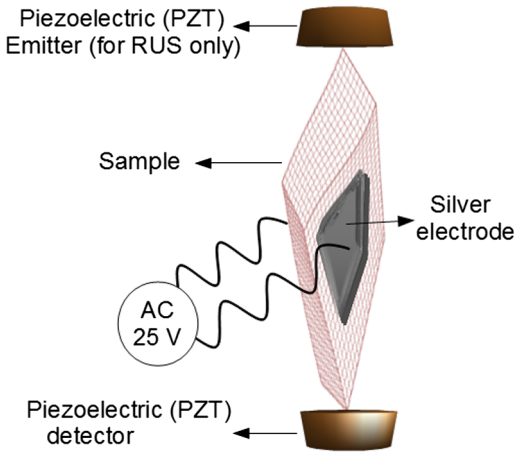

FIG. 1 (color online). Schematic diagram of the experimental arrangement for resonant piezoelectric spectroscopy (RPS). The same setup can be used for resonant ultrasonic spectroscopy (RUS) by applying the ac voltage across the top piezoelectric transducer rather than the electrodes coating two parallel surfaces of the sample. The applied ac voltage for RPS and RUS measurements on $SrTiO_3$ was 25 V.

We tested the novel RPS technique using the well-known ferroelectric material $BaTiO_3$ [21]. RPS measurements have found that the signals are very strong in the ferroelectric phase and that additional strong signals also appear as precursor effects above the transition point between the cubic and tetragonal phase. RPS amplitudes of mechanical resonances of $BaTiO_3$ at room temperature are larger than those in $SrTiO_3$ at low temperatures by more than 2 orders of magnitude. Such an enormous difference in amplitude reflects the fact that $BaTiO_3$ possesses a macroscopic polar order whereas $SrTiO_3$ is polar only at the nanoscale, i.e., in its ferroelastic domain walls. In addition, we compared the sensitivity of RPS with second harmonic generation (SHG) and found that RPS is slightly more sensitive than SHG [22]. Based on this observation we are confident that RPS does indeed allows us to study collective polarity, namely the generation of standing elastic waves by weak electric fields.

The sample of $SrTiO_3$ used in RPS and RUS experiments was a single crystal cut in the shape of a rectangular parallelpiped with dimensions of $5.107 \times 2.654 \times 3.229$ mm^3 [23]. For RPS measurements, the largest parallel surfaces were covered with silver paste to apply an ac voltage of 25 V across the sample. To switch from RPS to RUS experiments, the ac voltage was applied across the top transducer (Fig. 1). Each spectrum collected with RPS or RUS contained 50 000 data points between 20 kHz and 1.2 MHz. Data were collected in heating sequences using a low temperature cryogenic system described elsewhere [24]. RUS peak frequencies of selected resonance peaks were determined using an asymmetric Lorentzian profile. For RPS, frequencies were determined manually due to the sharp Fano profiles of mechanical resonances [25,26]. In addition, peak amplitudes (in volts) were determined manually, i.e., by subtracting the maximum point of the

resonance profile from the minimum point. A similar approach was used for RUS peak amplitudes.

RPS spectra, collected between 15 K and 100 K [Fig. 2(a)] display 5 peaks. In Fig. 2(a), we show, as an example, two resonance features with a Fano-like profile located around $\nu_1 \approx 40$ kHz and $\nu_2 \approx 85$ kHz. Upon heating, the amplitudes of both features decrease and disappear above $T^* \approx 80$ K as shown in Figs. 2(b) and 2(c). The detailed temperature dependencies of frequencies are different for these peaks. ν_1 decreases continuously on heating up to ≈ 80 K while ν_2 shows strong intensities only below 35 K. In order to identify these features, we performed RUS experiments. As shown in Fig. 2(d), two mechanical resonance peaks are also visible in RUS spectra for temperatures between 15 K and 120 K. Figure 3 shows the temperature dependence of the squared frequencies of the resonances; an important point to emphasize with respect to Fig. 3 is that below T^* the temperature dependence of the piezoelectric response exactly matches that of the resonant ultrasonic response; since the latter is a purely bulk property, the piezoelectric resonance cannot arise from surface effects [27]. A noticeable difference between ν_1 and ν_2 is their temperature dependence which is due to their respective effective elastic constants. The square of a resonant frequency is proportional to the effective elastic constant associated with that mode, which is usually a combination of bulk and shear elastic constants [19]. The resonance modes are dominated by shear waves, however. The temperature evolution of ν_1^2 at T_c suggests that ν_1 mainly depends on the elastic constant combination $C_{11} - C_{12}$ [23,28] while ν_2 depends primarily on C_{44} [23,28].

It is worth noting that RPS resonance frequencies and damping coefficients do not depend on experimental details while amplitudes depend on the position of the sample with respect to the acoustic receivers. This problem is the same as in RUS and amplitude measurements usually state whether a sample can be excited (rings) or not, while virtually no numerical amplitude data have ever been published for RUS. In this Letter we show such amplitude data (maximum of the piezoelectric receiver voltage at the resonance frequency) in Fig. 4 to demonstrate that the piezoelectric effect observed using RPS is comparable in their mechanical amplitudes to RUS amplitudes and is well outside the experimental error margins. The experimental error of the amplitude data is estimated to be around 10%. As shown in Fig. 4(a), the RPS amplitude of ν_1 starts to gradually increase upon cooling below T^* and peaks at $\approx$ 37 K, which is followed by another increase at $\sim$20 K. The RPS amplitude of ν_2 [Fig. 4(b)] is very small between T^*

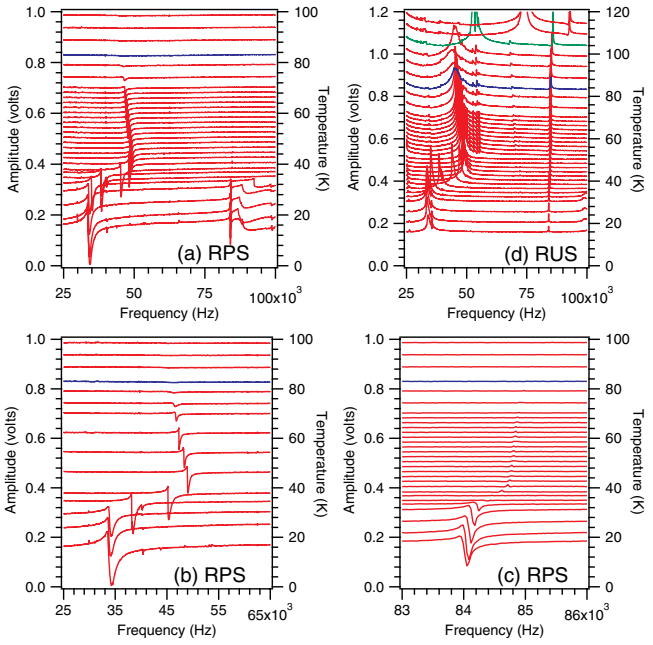

FIG. 2 (color online). Low temperature RPS and RUS spectra of $SrTiO_3$. Panel (a): Segments of RPS spectra in the frequency interval from 25 kHz to 100 kHz. The spectrum shown in blue was collected at $T^* \approx 80$ K. Disappearance of two mechanical resonances located at $\nu_1 \approx 40$ kHz and $\nu_2 \approx 85$ kHz with increasing temperature is shown in panels (b) and (c). Panel (d) shows segments of RUS spectra in the same frequency interval as in panel (a) for comparison. The spectrum shown in green was collected at the cubic-tetragonal ferroelastic transition temperature $T_c = 105$ K. In all panels the left axis represents the amplitude and the right axis gives the temperature at which each spectrum was collected.

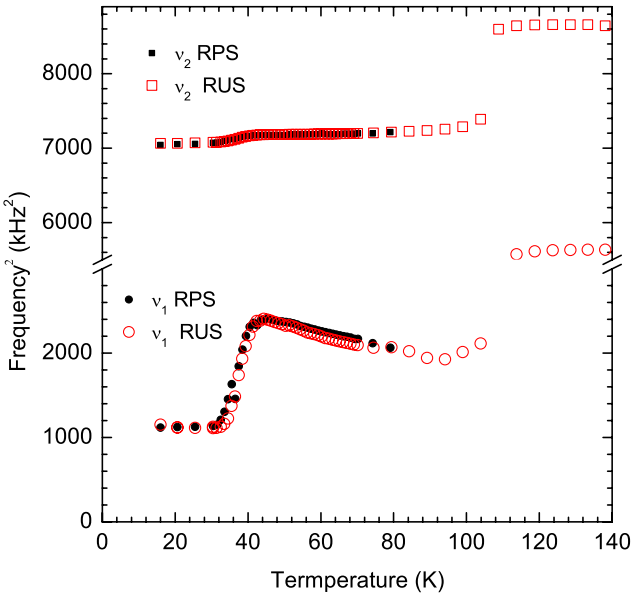

FIG. 3 (color online). The temperature evolution of the frequency of the mechanical resonance ν_1 (black, filled circles and empty, red circles) and ν_2 (black, filled squares and empty, red squares) determined using RPS and RUS. The agreement of results from RPS and RUS confirms that Fano-like features observed in the RPS spectra correspond to mechanical resonances of $SrTiO_3$, giving direct evidence of polarity in $SrTiO_3$.

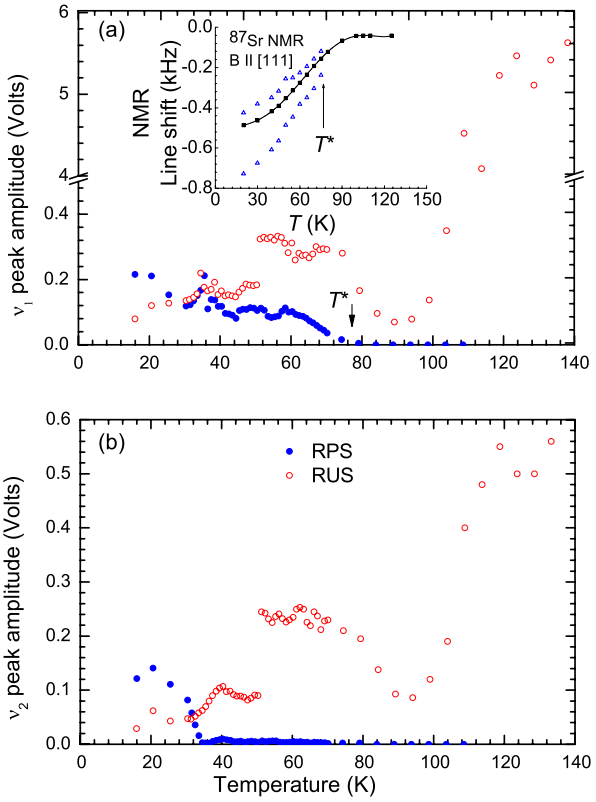

FIG. 4 (color online). The temperature evolution of the amplitudes of the mechanical resonances ν_1 and ν_2 observed using RPS and RUS measurements on $SrTiO_3$. (a) RPS (filled blue circles) and RUS (red empty circles) amplitudes of ν_1. The inset in part (a) shows the temperature dependence of the central $1/2 \leftrightarrow -1/2$ ^{87}Sr NMR transition at 9.2 T for $\mathbf{B} \parallel [111]$ in $SrTiO_3$ which is split into three components at $T < T^* \approx$ 75–80 K. The black squares represent the central NMR component that exhibits tetragonal symmetry whereas the triangles are the frequencies of satellite peaks, which exhibit nontetragonal symmetry. (b) RPS (filled blue circles) and RUS (red empty circles) amplitudes of ν_2. The uncertainty in RPS and RUS amplitudes is estimated to be 10%, which mainly stems from the mechanical coupling between the sample and transducers which may change by thermal contraction.

and $\approx$ 35 K and it rapidly increases at lower temperatures with a peak located around $\approx$ 20 K. RUS amplitudes of ν_1 and ν_2 are shown in Fig. 4 for comparison. A significant drop at T_c in the peak amplitudes is followed by a peak near 50 K, which clearly differs from the temperature evolution of the RPS amplitudes. The contrasting behavior of RPS and RUS amplitudes shows that the piezoelectric effect in $SrTiO_3$ is enhanced at low temperatures. The appearance of resonance modes in RPS spectra somewhat coincides with the temperature at which the central $1/2 \leftrightarrow -1/2$ ^{87}Sr NMR transition line of $SrTiO_3$ splits for a magnetic field of 9.2 T parallel to the [111] direction [6], which is presented in the inset of Fig. 4(a) (see Supplemental Material for experimental details of NMR measurements and data analysis [29]). The central ^{87}Sr NMR line starts to shift at $T_c = 105$ K. As resonances of all tetragonal domains coincide for $\mathbf{B} \parallel [111]$, there is a single NMR line between 105 K and $\approx$ 80 K. Below 75–80 K, the ^{87}Sr NMR line splits, demonstrating the triclinic local distortions of the lattice in the vicinity of Sr ions. Note that all the work we report in the present Letter is for normal O-16 isotopic $SrTiO_3$; while Blinc *et al.* emphasized the O-18 material [6], we use here only NMR data on the O-16 isotopic compound [29].

The present work reveals an unexpected novelty in that the material is polar, but only on the nanoscale and not as a bulk homogeneous property. The polarity is limited to domain walls, and its onset (at $\approx T^*$) correlates reasonably well with local triclinic distortions most probably related to the Sr-ion displacements along [111] directions measured by ^{87}Sr NMR [6,29]. Here, the temperature T^* is not well defined because we are not dealing with a bulk collective transition. Increases in RPS peak amplitudes with decreasing temperature suggest that the onset of polarity in the domain walls is gradual and that the high twin boundary mobility appears only after a minimum amount of polarity is accumulated in the twin walls. The difference between the temperature dependencies of RPS amplitudes can be explained by the respective effective elastic moduli of the resonances ν_1 and ν_2, $C_{11} - C_{12}$ and C_{44}. At temperatures above T_c, the resonance ν_1 was observed with weak amplitudes. We attribute its existence above T_c to flexoelectric effects [16]. Taking into account that the ratio of RUS to RPS amplitudes of the resonance ν_1 above T_c is an order of magnitude larger than the ratio below T_c, one can see the aforementioned flexoelectric effects are very weak compared to the piezoelectric effect in the ferroelastic domain walls below T^*.

The observed onset of polarity related to twin walls was predicted by Morozovska *et al.* [30] based on the coupling between the gradient of the ferroelastic order parameter and the polar displacement. The same effect was also predicted by biquadratic coupling between two order parameters, namely the tilt and the polarization [31,32]. The difference between the two coupling schemes is related to an artifact of the continuum approximation: only a few atomic layers inside the twin walls will be affected by the coupling. These atoms are either identified by a vanishing ferroelastic strain (biquadratic order parameter coupling) [31,32] or by a large spatial gradient of the same strain (gradient coupling) [30]. The small number of wall atoms can be described by several analytical functions which all relate to the same physical displacements of the polar mode. It is no surprise that the various coupling schemes lead to very similar results. The elastic effect of the antiphase boundaries is much smaller and not expected to excite mechanical resonances in RPS.

In summary, we report a new experimental method to detect standing elastic waves induced by piezoelectricity. Piezoelectricity is observed below 80 K and becomes

strong below 40 K. The elastic standing waves are driven by oscillation of polar twin boundaries. The demonstration of piezoelectricity in domain walls using RPS opens the door for systematic investigation of polar domain boundaries and represents a major step forward in the production and engineering of domain boundaries as functional structural elements [12]. These results also may affect the detailed modeling of superconductivity in strontium titanate [9]. They confirm a symmetry lower than the long-accepted $D4h$; they imply a very large increase in phonon density of states below ~50 K; they support a crystal field splitting of light and heavy electron bands; and they show that due to local polarity, spin-triplet superconductivity is most likely.

E. K. H. S. is grateful to EPSRC (RG66344) and the Leverhulme Foundation (RG66640) for support. RUS facilities in Cambridge were established through support from the NERC (NE/B505738/1) to M. A. C.

*es10002@cam.ac.uk

[1] K. A. Müller, W. Berlinger, and E. Tosatti, Z. Phys. B **84**, 277 (1991).
[2] O.-M. Nes, K. A. Müller, T. Suzuki, and F. Fossheim, Europhys. Lett. **19**, 397 (1992).
[3] E. Courtens, Ferroelectrics **183**, 25 (1996).
[4] B. Hehlen, A.-L. Pérou, E. Courtens, and R. Vacher, Phys. Rev. Lett. **75**, 2416 (1995).
[5] A. Koreeda, R. Takanao, and S. Saikan, Phys. Rev. Lett. **99**, 265502 (2007).
[6] R. Blinc, B. Zalar, V. V. Laguta, and M. Itoh, Phys. Rev. Lett. **94**, 147601 (2005).
[7] P. A. Fleury, J. F. Scott, and J. M. Worlock, Phys. Rev. Lett. **21**, 16 (1968).
[8] H. Q. Yuan, D. F. Agterberg, N. Hayashi, P. Badica, D. Vandervelde, K. Togano, M. Sigrist, and M. B. Salamon, Phys. Rev. Lett. **97**, 017006 (2006).
[9] X. Lin, Z. Zhu, B. Fauqué, and K. Behnia, Phys. Rev. X **3**, 021002 (2013).
[10] A. V. Kityk, W. Schranz, P. Sondergeld, D. Havlik, E. K. H. Salje, and J. F. Scott, Phys. Rev. B **61**, 946 (2000).
[11] R. J. Harrison, S. A. T. Redfern, and E. K. H. Salje, Phys. Rev. B **69**, 144101 (2004).
[12] E. K. H. Salje, ChemPhysChem **11**, 940 (2010).
[13] S. Van Aert, S. Turner, R. Delville, D. Schryvers, G. Van Tendeloo, and E. K. H. Salje, Adv. Mater. **24**, 523 (2012).
[14] L. Goncalves-Ferreira, S. A. T. Redfern, E. Artacho, and E. K. H. Salje, Phys. Rev. Lett. **101**, 097602 (2008).
[15] J. Petzelt, T. Ostapchuk, I. Gregora, I. Rychetský, S. Hoffmann-Eifert, A. V. Pronin, Y. Yuzyuk, B. P. Gorshunov, S. Kamba, V. Bovtun, J. Pokorný, M. Savinov, V. Porokhonskyy, D. Rafaja, P. Vaněk, A. Almeida, M. R. Chaves, A. A. Volkov, M. Dressel, and R. Waser, Phys. Rev. B **64**, 184111 (2001).
[16] P. Zubko, G. Catalan, P. R. L. Welche, A. Buckley, and J. F. Scott, Phys. Rev. Lett. **99**, 167601 (2007).
[17] A. Erba, K. E. El-Kelany, M. Ferrero, I. Baraille, and M. Rérat, Phys. Rev. B **88**, 035102 (2013).
[18] D. Wang, E. K. H. Salje, S.-B. Mi, C.-L. Jia, and L. Bellaiche, Phys. Rev. B **88**, 134107 (2013).
[19] A. Migliori and J. Sarrao, *Resonant Ultrasound Spectroscopy: Applications to Physics, Materials Measurements, and Nondestructive Evaluation* (Wiley, New York, 1997).
[20] E. K. H. Salje, M. A. Carpenter, G. F. Nataf, G. Picht, K. Webber, J. Weerasinghe, S. Lisenkov, and L. Bellaiche, Phys. Rev. B **87**, 014106 (2013).
[21] O. Aktas, M. A. Carpenter, and E. K. H. Salje, Appl. Phys. Lett. **103**, 142902 (2013).
[22] A. M. Pugachev, V. I. Kovalevskii, N. V. Surovtsev, S. Kojima, S. A. Prosandeev, I. P. Raevski, and S. I. Raevskaya, Phys. Rev. Lett. **108**, 247601 (2012).
[23] J. F. Scott, E. K. H. Salje, and M. A. Carpenter, Phys. Rev. Lett. **109**, 187601 (2012).
[24] R. E. McKnight, M. A. Carpenter, T. W. Darling, A. Buckley, and P. A. Taylor, Am. Mineral. **92**, 1665 (2007).
[25] U. Fano, Phys. Rev. **124**, 1866 (1961).
[26] D. J. Safarik, E. K. H. Salje, and J. C. Lashley, Appl. Phys. Lett. **97**, 111907 (2010).
[27] A. Kholkin, I. Bdikin, T. Ostapchuk, and J. Petzelt, Appl. Phys. Lett. **93**, 222905 (2008).
[28] M. A. Carpenter, Am. Mineral. **92**, 309 (2007).
[29] See Supplemental Material at http://link.aps.org/supplemental/10.1103/PhysRevLett.111.247603 for NMR spectra collected between 20 K and 105 K and their analysis.
[30] A. N. Morozovska, E. A. Eliseev, M. D. Glinchuk, L.-Q. Chen, and V. Gopalan, Phys. Rev. B **85**, 094107 (2012).
[31] B. Houchmandzadeh, J. Lajzerowicz, and E. Salje, J. Phys. Condens. Matter **3**, 5163 (1991).
[32] S. Conti, S. Müller, A. Poliakovsky, and E. K. H. Salje, J. Phys. Condens. Matter **23**, 142203 (2011).